

The Role of Specific Amino Acid Residues in The Vibrational Properties of Plastocyanin

E. Fraga and G. R. Loppnow*

Department of Chemistry, University of Alberta, Edmonton, Alberta T6G 2G2, Canada

Received: December 18, 2001; In Final Form: May 9, 2002

Resonance Raman spectra for zucchini, cucumber, bean, and lettuce plastocyanins, blue copper proteins involved in plant photosynthetic electron transport, have been measured at wavelengths throughout their intense 600-nm absorption band. A comparison of the resonance Raman spectra of these four plastocyanins, and two others previously quantified, demonstrates that they all exhibit vibrational bands with similar frequencies but significantly different relative intensities. Self-consistent analysis of the absorption band and resulting resonance Raman excitation profiles using a time-dependent wave packet formalism for these four plastocyanins demonstrates that many of the derived molecular parameters are similar to those determined previously for two other species of plastocyanin. However, significant differences are observed in the mode-specific displacements and reorganization energies, although the total reorganization energy is 0.16 ± 0.01 eV for all six plastocyanins. A detailed comparison of the structural and compositional differences among the six plastocyanins, using the previously reported structure of poplar *a* plastocyanin, suggests that these mode-specific differences arise from specific amino acid differences within 10–12 Å of the copper site. These results are interpreted as arising from a through-bond mode-mixing mechanism and a through-space electrostatic mechanism and suggest that the normal modes of the copper site are delocalized into the protein. In addition, lettuce plastocyanin has a significantly greater homogeneous line width, probably as a result of compositional differences adjacent to the copper active site. These results demonstrate that the protein environment is strongly coupled to or mixed in with the copper site vibrational dynamics. Further evidence for the sensitivity of the resonance Raman intensities to particular electron-transfer pathways within the protein is also discussed.

Introduction

The rate constant for charge or electron transfer can be described by the Marcus equation:^{1–4}

$$k_{\text{ET}} \propto H_{\text{AB}}^2 \exp\{-(\Delta G^\circ + \lambda)^2/(4\lambda RT)\} \quad (1)$$

where ΔG° is the free energy change upon electron transfer, λ is the reorganization energy, T is the temperature, and H_{AB} is the electronic coupling between donor and acceptor. The reorganization energy is usually written as the sum of the inner and outer sphere contributions ($\lambda = \lambda_i + \lambda_o$), where λ_i is loosely defined as the structural reorganization of the donor and acceptor (nuclear) conformation, and λ_o is defined as the structural reorganization of the solvent (electronic and nuclear) conformation to the new electronic distribution. The solvent or protein environment may affect the free energy change, the reorganization energy, or the coupling strength or a combination of these.

Considerable research effort has been expended on determining how the protein environment modulates electron transfer within and between active sites in proteins. For example, significant changes in the rate of electron transfer are observed upon selective introduction of point charges in the bacterial photosynthetic reaction center;⁵ indeed, electron transfer can even be induced along the physiologically silent “M path” by introduction of a positively charged lysine near the M-side bacteriochlorophyll and replacement of the L-side bacteriopheophytin with bacteriochlorophyll.⁵ In azurin, a blue copper protein

similar in structure and function to the plastocyanins studied here, significant changes in electron-transfer rate constants are also observed upon amino acid substitutions along the electron-transfer pathway.⁶

Plastocyanin is a 10 500-Da Type I “blue” copper protein that acts as an electron transport agent between cytochrome *f* and photosystem I in plant photosynthesis and exhibits a strong absorption band centered at ca. 600 nm.⁷ Previous studies^{8,9} have shown that this Cu site $\pi\pi^*$ transition is strongly coupled to the electron transfer and could provide a good model for understanding the electron-transfer pathway. In previous papers,^{10–12} we have demonstrated that the Raman intensities, which are resonance-enhanced by this absorption band, provide a unique probe of vibrational mixing within plastocyanin. By using the resonance Raman intensities, fluorescence spectrum, absorption spectrum, X-ray crystal structure, and molecular modeling, we showed that amino acids up to 8–10 Å away are coupled to the electronic transition at the copper active site.^{11,12} The primary goal of this previous work^{10–12} was to determine the mode-specific dynamics in a model system in which the chromophore has a well-defined structure and sits in a relatively isolated, well-characterized environment. Plastocyanin is a particularly useful model of solvent–solute interactions because the structure of the protein is well established¹³ and because the copper ion is buried among hydrophobic amino acid residues in one end of the protein and does not show any external solvent accessibility.^{13,14} Because of the lack of solvent accessibility in plastocyanin, the protein plays the role of the solvent. It was found that the protein environment contributes to the total excited-state reorganization energy in two ways, a mode-specific component from the resonance-enhanced vibrations and a bulk-

* To whom correspondence and reprint requests should be addressed.
E-mail: glen.loppnow@ualberta.ca. WWW page: <http://www.chem.ualberta.ca/~gloppnow>.

solvent-like dephasing component as evidenced by the homogeneous line width.¹⁰ Only the mode-specific component was found to be dependent on the amino acid composition of plastocyanin.

In this paper, we extend these studies to examine more closely the role of environment on the resonance Raman spectra by comparing the Raman-derived molecular parameters for the 600-nm $\pi\pi^*$ transition in six plastocyanins: poplar *a*, spinach, lettuce, zucchini, cucumber, and bean. Determination of the molecular parameters in zucchini, cucumber, lettuce, and bean plastocyanins allows us to examine the role of amino acid composition at both shorter and longer distances from the copper site, as well as to explore in more detail the proposed through-space and through-bond mixing/coupling mechanisms. The high homology among the primary sequences of the six plastocyanins studied here allows relationships to be established between the observed mode-specific reorganization energies and specific structural or electrostatic characteristics or both of the plastocyanins. An important result is that the mode-specific molecular distortions among the six plastocyanins are particularly sensitive to specific amino acid substitutions around the chromophoric copper site via normal modes delocalized into the protein backbone, although the total reorganization energy remains constant. These results are discussed with respect to the ground-state normal modes and excited-state distortions of plastocyanin.

Experimental Section

Materials. Isolation of zucchini, cucumber, and bean plastocyanin was accomplished by using a procedure similar to that used for parsley and poplar plastocyanin.^{10,11,15,16} Briefly, 5 kg of leaves, from plants grown locally, were homogenized in small batches with 4.5 kg of crushed ice, 500 mL of Tris-HCl pH 7.6, and 5 L of cold acetone. The precipitated proteins were collected, dialyzed, and purified as described previously.^{10,11} The yield was 37, 21, and 20 mg plastocyanin/kg leaves with purity ratios $A_{278}/A_{597} = 1.14, 1.3, \text{ and } 1.3$ for zucchini, cucumber, and bean plastocyanins, respectively. These purity ratios are close to the literature values^{13,17} of 1.0–1.2, 1.1, and 1.2, respectively.

Plastocyanin was isolated from lettuce leaves according to a previously published procedure,¹⁸ and this procedure was similar to the protocol used for isolation of spinach plastocyanin.¹¹ Briefly, 5 kg of lettuce leaves ("green leaf" variety, purchased locally) were homogenized with 6 L of sucrose buffer (0.4 M sucrose, 50 mM KCl, 50 mM Tris-HCl, pH 8.0). After filtration and centrifugation, the resulting chloroplast pellet was resuspended in Tris-HCl (400 mL, pH 8.0) and precipitated with cold acetone to a concentration of 35% (v/v). The precipitate was centrifuged and discarded. More acetone was added to the supernatant to a final concentration of 80% (v/v). Purification of the resulting plastocyanin precipitate was performed as previously described.^{10,11} Yields were variable, 2–6 mg plastocyanin/kg leaves with an average purity ratio $A_{278}/A_{597} = 1.44$, close to the literature value¹⁷ of 1.2.

Spectroscopy. Room-temperature resonance Raman spectra of plastocyanin were obtained and analyzed as previously described.^{10,11} Briefly, 60–100 mW of the exciting laser was focused to a 100- μm diam spot on a 5-mm o.d. spinning NMR tube containing the plastocyanin solution. Resonance Raman spectra were obtained in a 135° backscattering geometry at a resolution of 5–7 cm^{-1} by using a CCD detector coupled to a single monochromator. Frequency calibration was performed by obtaining spectra of three solvents (chloroform, carbon tetrachloride, and benzene) of which the Raman frequencies are

known. Reported frequencies are accurate to $\pm 2 \text{ cm}^{-1}$. Bleaching of the sample was accounted for by measuring the absorbance at 700 nm before and after each scan ($\epsilon = 1295 \text{ cm}^{-1} \text{ M}^{-1}$). The average absorbance was used to determine the concentration of plastocyanin. The observed bleaching in a 90 min scan was $\leq 7\%$, suggesting that the bulk and single-pass photoalteration parameters are small.^{10,11,19} Measurement of the resonance Raman spectrum and determination of the intensities were repeated on three fresh samples of plastocyanin for each excitation wavelength. The methods used here for converting the resonance Raman intensities of plastocyanin into absolute cross sections¹⁰ and for correcting for self-absorption effects¹⁹ have been described previously. The cross sections of cacodylate used in the determination of absolute cross sections were calculated as described previously.¹⁰

Theory. The absorption and resonance Raman cross sections in the Condon approximation can be written using the time-dependent formalism of Lee and Heller:^{20,21}

$$\sigma_A = \frac{4\pi e^2 M^2 E_L}{6\hbar^2 c n} \int_0^\infty P(E_0) dE_0 \int_{-\infty}^\infty \langle i|i(t) \rangle e^{i(E_L + \epsilon_i)t/\hbar} G(t) dt \quad (2)$$

$$\sigma_R = \frac{8\pi E_S^3 E_L e^4 M^4}{9\hbar^6 c^4} \int_0^\infty P(E_0) dE_0 \times \left| \int_0^\infty \langle f|i(t) \rangle e^{i(E_L + \epsilon_i)t/\hbar} G(t) dt \right|^2 \quad (3)$$

where E_L and E_S are the energies of the incident and scattered photons, respectively, n is the refractive index, M is the transition length, ϵ_i is the energy of the initial vibrational state, $|i\rangle$ and $|f\rangle$ are the initial and final vibrational wave functions, $G(t)$ is the homogeneous line width function, and $|i(t)\rangle = e^{-i2\pi H t/\hbar} |i\rangle$ is the initial ground vibrational wave function propagated on the excited electronic state potential surface. $P(E_0)$ is a Gaussian distribution of zero-zero energies, representing inhomogeneous site broadening.²⁰ The general implementation of these equations has been described in detail,²⁰ as has their specific application to parsley, poplar *a*, and spinach plastocyanins.^{10,11} The parameters for poplar *a* plastocyanin^{10,11} were used as a starting point for the four plastocyanins analyzed here. All eight observed fundamental vibrational modes were used in the time-dependent calculations. The relative Δ 's were scaled to give the experimentally observed absorption and resonance Raman excitation profile bandwidths. The homogeneous line width (Γ) was determined primarily by the absolute magnitudes of the resonance Raman excitation profiles. No inhomogeneous broadening in any of the plastocyanins, as determined experimentally by the absorption and resonance Raman excitation profile band shapes, was necessary to reproduce the observed spectral data. The transition length (M) and the energy gap between potential surfaces (E_0) were determined by the magnitude and position of the absorption spectrum, respectively. These parameters were optimized iteratively until the calculated and experimental absorption spectrum and resonance Raman excitation profiles were in agreement.

Results

A comparison of the resonance Raman spectra of six plastocyanins is shown in Figure 1. The poplar *a* and spinach plastocyanin resonance Raman spectra are identical to the previously reported spectra.^{11,12,22} The cacodylate vibrations, used as the intensity standard, are visible as a pair of bands centered at 603 and 638 cm^{-1} . Approximately six intense bands

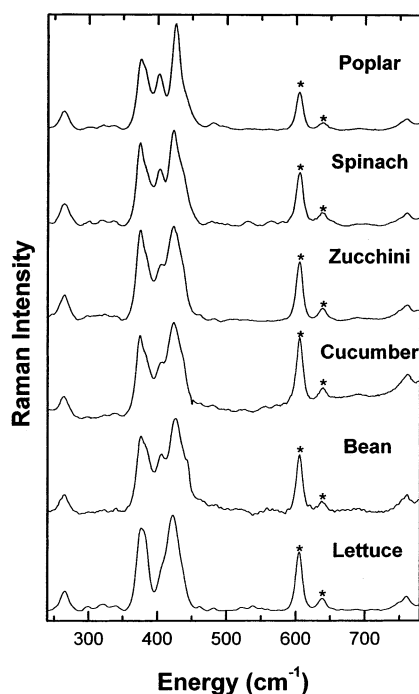


Figure 1. Resonance Raman spectra of 0.7–1 mM poplar *a*, spinach, zucchini, cucumber, bean, and lettuce plastocyanin excited at 568 nm. The spectra are the sum of three to nine scans and have been divided by a tungsten–halogen lamp spectrum. The cacodylate intensity standard vibrations (*) appear at 603 and 638 cm^{-1} .

are observed between 350 and 500 cm^{-1} and have been previously assigned to normal modes involving the Cu–S stretch mixed with other internal coordinates,^{9,22–28} primarily those of the cysteinate ligand, although the exact assignments are still controversial. The moderately intense bands at 263 and 760 cm^{-1} have previously been assigned to the symmetric Cu–N stretch from the histidine ligand(s) and the C–S stretch of the cysteinate ligand, respectively.²³ A broad band centered at 824 cm^{-1} (data not shown) arises from combination and overtone transitions of the vibrations between 350 and 500 cm^{-1} and also contains a contribution from the broad 825 cm^{-1} As=O stretch of the cacodylate internal standard.^{29,30}

Figure 2 shows a detailed comparison of the resonance Raman spectra of the six plastocyanins in the 300–500 cm^{-1} region. A quick glance at the spectra demonstrates that many of the spectral features are similar. Many of the frequencies coincide within the $\pm 2 \text{ cm}^{-1}$ experimental error. This result is particularly true for zucchini, cucumber, bean, and lettuce plastocyanin. The intensities are also similar for the poplar *a*, spinach, zucchini, cucumber, and bean plastocyanin. However, a detailed examination of the spectra reveals significant differences in relative intensities among the spectra of the six plastocyanins. This result is particularly true for lettuce plastocyanin, compared to the other five (Figure 1), and suggests different mode-specific descriptions of their excited-state dynamics. For example, the intensity of the 405 cm^{-1} peak of lettuce plastocyanin is approximately 60% of the intensity of the 403 cm^{-1} peak of bean plastocyanin. As described^{10–12,19} in previous comparisons of plastocyanin and azurin spectra, the resonance Raman spectrum obtained for each species was unaffected by protein preparation, excitation wavelength, and ionic strength. Figure 2 also shows the decomposition of the spectrum into its component peaks and the resulting fit to the experimental resonance Raman spectrum for the four plastocyanin species treated quantitatively in this paper. For this decomposition, the bandwidth and band shape were kept constant to better examine the spectral intensity

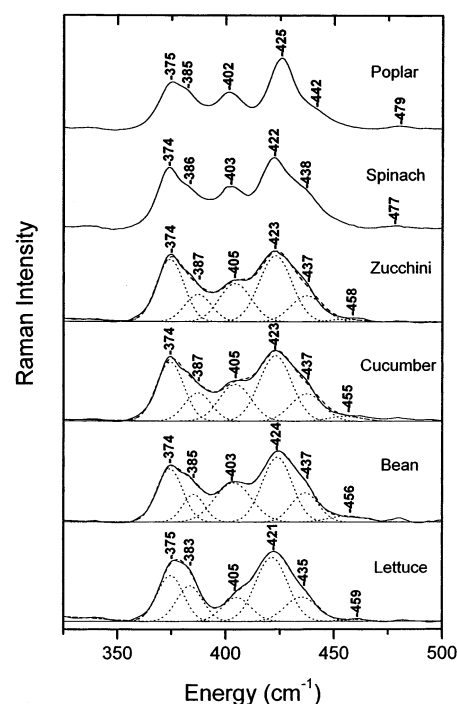


Figure 2. Experimental resonance Raman spectra (solid lines) in the 300–500 cm^{-1} region of 0.7–1 mM poplar *a*, spinach, zucchini, cucumber, bean, and lettuce plastocyanin excited at 568 nm. The spectra are the sum of three to nine scans and have been divided by a tungsten–halogen lamp spectrum. Decompositions of the zucchini, cucumber, bean, and lettuce spectra into their component peaks (dotted lines) are shown, and the sums of the component peaks (dashed lines) are shown. Note the similar vibrational frequencies but significantly different relative intensities of particular peaks among the six spectra.

differences; only the frequency and height were allowed to vary. In all four spectra, the fits follow the experimental spectrum well and show no evidence of missing or extra peaks.

Figures 3–5 illustrate the good agreement between the experimental and calculated resonance Raman excitation profiles and absorption spectra of zucchini, cucumber, lettuce, and bean plastocyanin using the parameters summarized in Tables 1 and 2. The discrepancy between the observed and simulated absorption spectra is due to other electronic transitions within the 600-nm absorption band^{10,11} and is consistent with a previous Stark study³¹ of the electronic structure in plastocyanin. The experimental excitation profiles of the observed modes in all four species have similar shapes and, as observed^{10,11} before for spinach and poplar *a* plastocyanin, are somewhat narrower than the absorption spectrum, consistent with more than one electronic transition in this absorption band. These similarities in shape are borne out by the similarity in molecular excited-state parameters (Table 2) for the six species of plastocyanin compared here, particularly for those parameters that describe only the electronic characteristics of the excited state (e.g., transition length and zero–zero energy). The absorption spectra of plastocyanin from the four species are essentially superimposable (Figure 5), demonstrating that the electronic character of the excited state is similar in the four plastocyanins. This last result is consistent with the results of Stark spectroscopy³¹ of different species of azurin, which showed little variation of the electronic structure with species. Also, the total absolute resonance Raman cross sections, integrated over all of the observed vibrational bands, are the same within experimental error, indicating that the total reorganization energy is similar for the six plastocyanins. The total inner-sphere reorganization energy for each plastocyanin can be calculated from the values

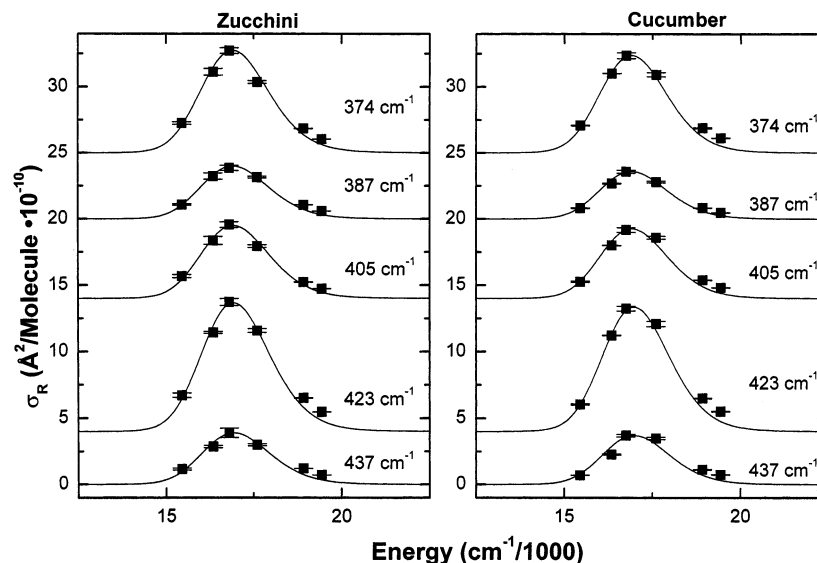


Figure 3. Experimental (points) and calculated (solid line) resonance Raman excitation profiles of the five most intense modes of zucchini (left) and cucumber (right) plastocyanin. The excitation profiles were calculated with eq 3 by using the parameters of Tables 1 and 2. Error bars represent the uncertainties in the absolute resonance Raman cross sections. The excitation profiles have been offset along the ordinate for greater clarity of presentation.

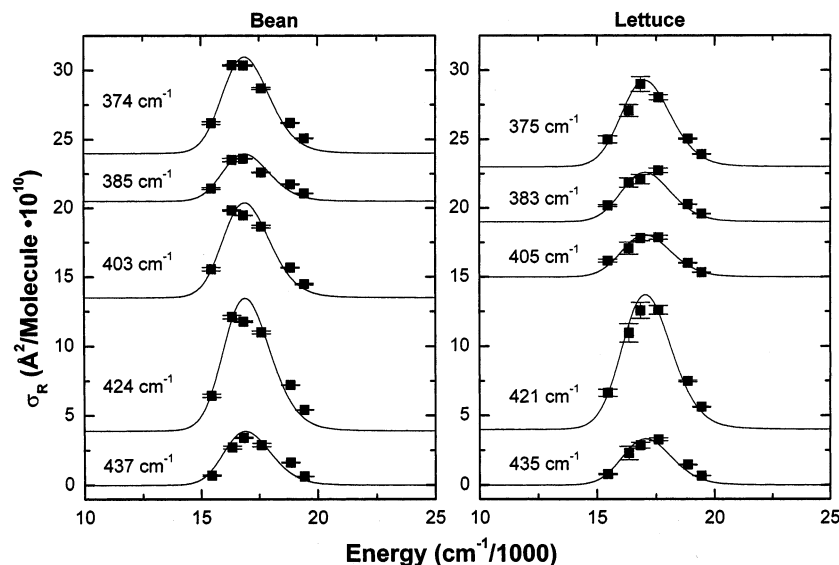


Figure 4. Experimental (points) and calculated (solid line) resonance Raman excitation profiles of the five most intense modes of bean (left) and lettuce (right) plastocyanin. The excitation profiles were calculated with eq 3 by using the parameters of Tables 1 and 2. Error bars represent the uncertainties in the absolute resonance Raman cross sections. The excitation profiles have been offset along the ordinate for greater clarity of presentation.

TABLE 1: Harmonic Mode Parameters of Poplar *a*, Spinach, Zucchini, Cucumber, Lettuce, and Bean Plastocyanins^a

poplar <i>a</i>		spinach		zucchini		cucumber		bean		lettuce	
mode (cm ⁻¹)	Δ	mode (cm ⁻¹)	Δ	mode (cm ⁻¹)	Δ	mode (cm ⁻¹)	Δ	mode (cm ⁻¹)	Δ	mode (cm ⁻¹)	Δ
263	0.87	263	0.89	264	0.93	264	0.93	263	0.86	266	0.96
375	1.13	374	1.14	374	1.22	374	1.18	374	1.21	375	1.19
385	1.08	386	0.96	387	0.85	387	0.80	385	0.83	383	0.88
402	1.00	403	0.98	405	0.96	405	0.93	403	1.12	405	0.77
425	1.59	422	1.26	423	1.22	423	1.18	424	1.26	421	1.32
442	0.75	438	1.07	437	0.75	437	0.73	437	0.78	435	0.75
480	0.25	478	0.30	458	0.32	456	0.29	456	0.35	459	0.31
760	0.31	760	0.34	756	0.35	756	0.31	760	0.34	756	0.36

^a Data for spinach and poplar *a* plastocyanin is from ref 11. Δ's are in units of dimensionless normal coordinates. The estimated error in the displacements is ±10%.

in Table 1 and from the relation $\lambda_{i,\text{total}} = \sum(\Delta_j^2 \omega_j)/2$ where the sum is carried out over all j normal modes, and these energies are given in Table 2. The average total reorganization energy is $1280 \pm 100 \text{ cm}^{-1}$ ($0.158 \pm 0.013 \text{ eV}$) over the six

plastocyanins. The small standard deviation indicates the similar reorganization energy among these plastocyanins. The similarity of the electronic parameters is also reflected in the identical homogeneous and inhomogeneous line widths used in the

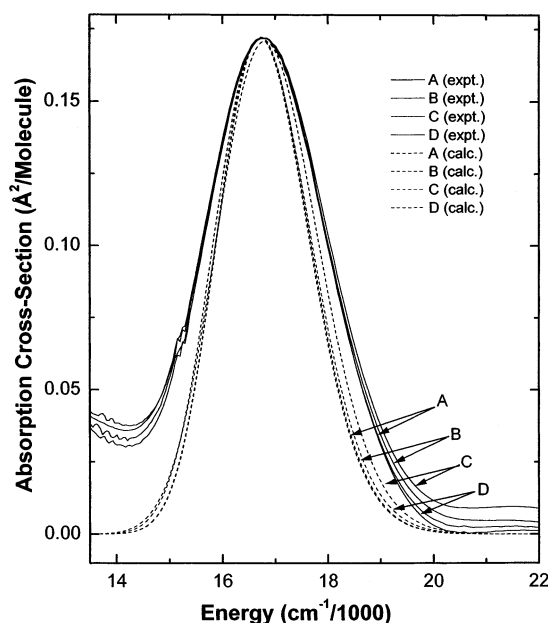


Figure 5. Experimental (solid lines) and calculated (dashed lines) absorption spectra of plastocyanins. Experimental and calculated spectra are shown for zucchini (A), cucumber (B), lettuce (C), and bean (D) plastocyanin. The calculated spectra are generated from eq 2 by using the parameters of Tables 1 and 2. Deviations of the calculated from the experimental absorption spectrum at higher and lower energies arise from other electronic transitions that were not modeled and that apparently contribute no resonance enhancement to the observed resonance Raman spectra.

TABLE 2: Excited-State Parameters for Poplar *a*, Spinach, Zucchini, Cucumber, Lettuce, and Bean Plastocyanins^a

parameter	poplar ^a	spinach ^b	zucchini ^c	cucumber ^c	bean ^c	lettuce ^c
E_0 (cm ⁻¹)	15 350	15 500	15 600	15 675	15 500	15 650
M (Å)	0.58	0.57	0.56	0.56	0.57	0.58
Γ_G (cm ⁻¹)	385	385	380	388	395	460
$\lambda_{i,\text{total}}$ (eV)	0.18	0.17	0.15	0.14	0.16	0.15

^a In this table, E_0 is the zero-zero energy, M is the transition length, Γ_G is the homogeneous line width of Gaussian line shape, and $\lambda_{i,\text{total}}$ is the total inner-sphere reorganization energy. ^b Values from ref 11. ^c Values from this work.

simulations for five of the six plastocyanins. Because the homogeneous line width reflects both the excited-state population relaxation time and the protein-induced broadening processes, these results suggest that the kinetics of population relaxation and the breadth of the solvent-induced distribution of zero-zero energies may also be similar among the different species of plastocyanin (vide infra).

As illustrated in Figure 2, the relative resonance Raman intensities vary with species. This modulation in the mode-specific description of the ground or excited state or both is directly reflected in the different experimental absolute resonance Raman cross sections (Figures 4 and 5) and excited-state geometry displacements (Table 1) in the six species for the same vibrational band (e.g., compare the excitation profiles for the 403 cm⁻¹ mode of bean and the 405 cm⁻¹ mode of lettuce plastocyanin in Figure 4). This difference is illustrated more clearly in Table 1, which presents the mode-specific excited-state displacements as a function of the species of plant from which the plastocyanin is obtained. This table shows that many of the excited-state displacements, except for the weak modes at ~480 and ~760 cm⁻¹, are significantly different in the six plastocyanins. The molecular origin of these intensity redistribu-

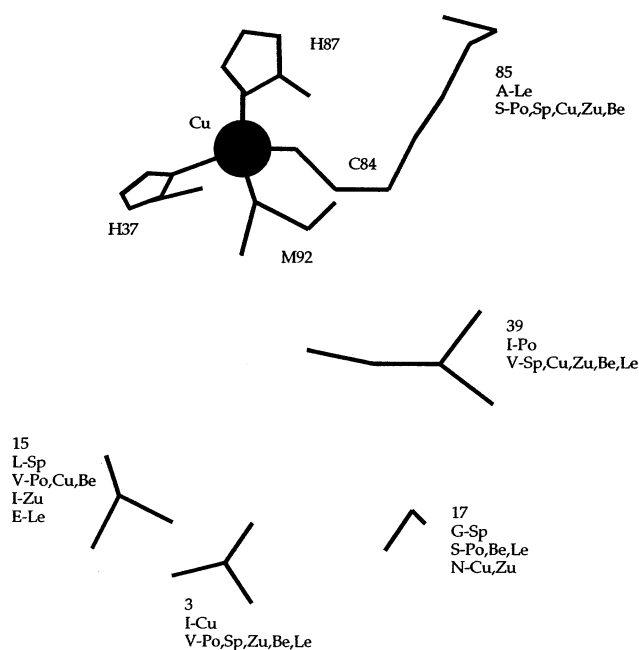


Figure 6. Scale line drawing of the copper site and selected amino acids of poplar *a* plastocyanin from the Protein Data Bank³⁵ crystallographic coordinates.³⁶ The copper ion is rendered as CPK type. The copper ligands are His37, Cys84, His87, and Met92. In the figure, the numbers represent the amino acid sequence number, the one-letter codes are given for the amino acid residues, and the 2-letter codes refer to the species of plastocyanin, where sp = spinach, po = poplar, zu = zucchini, cu = cucumber, be = bean, and le = lettuce.

tions, particularly in bean and lettuce plastocyanin, will be discussed below.

Discussion

The primary purpose of this paper is to explore the role of solvent on the vibrational dynamics by using a structurally well-defined solute and solvent, the blue copper protein plastocyanin. In a previous paper,¹² the resonance Raman spectra of four plastocyanins were compared. By performing the quantitative analysis of the resonance Raman intensities here and by including more species of plastocyanin, we can directly and more precisely compare the dynamics among the plastocyanins as a function of protein environment.

Much of the discussion below is couched in the terms of excited-state displacements, the Δ 's in Table 1, which are obtained in the harmonic approximation from the time-dependent model of resonance Raman intensities (eqs 2 and 3). The excited-state displacements represent the change in equilibrium geometry upon going from the ground to excited state and, thus, are sensitive to *both* the ground- and excited-state vibrational and electronic properties. Therefore, mechanisms that may affect both ground- and excited-state properties of plastocyanin must be considered.

Comparison of Plastocyanins. In previous papers,^{11,12} it has been noted that the resonance Raman spectra and resonance Raman-derived parameters of poplar *a* and spinach plastocyanin are significantly different. This result has been interpreted as arising from a differential composition-dependent mixing of internal coordinates in the two species; spinach and poplar *a* plastocyanins differ in amino acid composition at residue 39, 2 residues away from the coordinated His37 (Figure 6). In other words, the normal modes enhanced by the $\pi\pi^*$ electronic transition at the copper site are actually delocalized into the protein backbone via the coordinating residues and change their

character upon changes in protein composition. This interpretation is supported here by the observation that the resonance Raman spectra of zucchini and cucumber plastocyanin are essentially identical. This pair has the same amino acid difference at roughly the same through-space distance as the spinach/poplar *a* plastocyanin pair but at residues much further away along the peptide backbone (through-bond distance) from the Cu-coordinating residues. At the longer through-bond distances in zucchini/cucumber plastocyanin, mixing of internal coordinates is highly unlikely. The results presented in Tables 1 and 2 show that the excited-state parameters of zucchini and cucumber plastocyanin are also similar, as would be expected from the similar spectra. The excited-state displacements for zucchini and cucumber plastocyanin are the same within the 10% error, consistent with no significant changes in protein composition in this pair of plastocyanins that affect the resonance Raman spectra or the ground- or excited-state properties.

In a previous paper,¹² it was also noted that slight differences exist between the resonance Raman spectra of spinach and zucchini plastocyanin (see also Figure 2). Slight differences in frequency and a broader-appearing 422 cm⁻¹ peak in zucchini plastocyanin were attributed to the addition of a dipolar amino acid residue approximately 12 Å from the copper site on going from spinach to zucchini plastocyanin. This dipole appears to affect either the ground-state or excited-state potential energy surface, probably through some electrostatic effect.¹² Table 1 shows that the displacements of the 437 cm⁻¹ mode are ~40% different between spinach and zucchini plastocyanin, significantly outside the error limits of this analysis, suggesting that electrostatic mechanisms may act on vibrational properties in a mode-specific manner in anisotropic environments. However, more work is necessary to specifically test this hypothesis.

The spectra and quantitative analysis of two additional species of plastocyanin, from french bean and lettuce, provide a unique opportunity to test the hypotheses put forth in the previous papers^{11,12} regarding the effect of the protein environment on the resonance Raman intensities and resulting molecular parameters of the copper site chromophore. One unresolved issue was whether the observed spectral differences arise from specific amino acid residues or from the protein composition as a whole. For example, zucchini and cucumber plastocyanin have almost identical resonance Raman spectra and no significant amino acid differences within 10 Å of the copper site, as discussed above. However, they also share the highest overall protein composition identity, 91% identical amino acid residues between the two proteins. Measurement of the quantitative resonance Raman intensities of bean and lettuce plastocyanin allows us to show conclusively that these spectral differences arise from specific amino acid residues. Figures 1 and 2 clearly show that the resonance Raman spectra of bean and lettuce plastocyanin are significantly different, even though they share 88% identical amino acid residues. The spectrum of bean plastocyanin is much more similar to that of spinach (84% identity) and poplar *a* (79% identity) plastocyanin than that of lettuce plastocyanin. This discrepancy can be understood by examining the location and identity of the different amino acid residues among the four plastocyanins described here (Figure 6). Bean plastocyanin has the same amino acids as poplar *a* plastocyanin at all residues within 10 Å of the copper site except at residue 39, where a valine has been substituted for an isoleucine, similar to spinach plastocyanin. However, bean and lettuce differ significantly at residue 85 (Figure 6), directly adjacent to Cys84 where the electronic transition is localized, and at residue 15, much further

from the copper site. These spectral differences are also reflected in the displacements (Table 1). The displacement of the 403 cm⁻¹ mode for bean plastocyanin is significantly different from the displacement of the 405 cm⁻¹ mode for lettuce plastocyanin.

The uniquely different resonance Raman spectrum and resulting molecular parameters of lettuce plastocyanin require further comment. The resonance Raman spectrum of lettuce plastocyanin has a shifted 405 cm⁻¹ band, an almost complete lack of intensity around 395 cm⁻¹, and equal-intensity bands at 375 and 384 cm⁻¹, features that do not occur in the resonance Raman spectra of any other plastocyanin presented here (Figures 1 and 2). Furthermore, the homogeneous line width of lettuce plastocyanin is significantly larger than any other plastocyanin measured thus far. Again, a look at the amino acid residues surrounding the copper site in plastocyanin provides an explanation for these spectral anomalies in lettuce plastocyanin. As Figure 6 shows, only lettuce plastocyanin has a significantly different residue directly adjacent to an amino acid ligand of the copper ion; lettuce contains an alanine at position 85, while all of the other plastocyanins studied have a serine residue at this position. In addition, lettuce has an additional charge within 10 Å of the copper site compared to all of the other plastocyanins; residue 15 is an aspartate in lettuce plastocyanin, while all of the other plastocyanins studied have an aliphatic side chain at this position. These two amino acid changes are much more significant changes in chemical properties than the differences between any other pairs of plastocyanins studied here. Thus, they should also have a proportionately larger influence on the spectral properties. *In conclusion, it is the location and physical properties of the amino acids within ~10 Å of the copper site that influence the resonance Raman intensities and resulting molecular parameters.*

Local vs Delocalized Normal Modes. A remaining issue is whether the long-range effects on the resonance Raman spectra of plastocyanins observed here are ground-state or excited-state effects. For the reasons enumerated below, we believe that the effects are primarily ground-state effects. The spectral intensity differences observed here are usually accompanied by frequency changes, particularly when the intensity differences are large, supporting the suggestion that these arise from a composition-dependent mixing of internal coordinates to form the ground-state normal modes.^{11,12} We have also measured the combination and overtone band intensities in the 700–900 cm⁻¹ region with 597 nm excitation as an additional check on the excited-state frequencies used in the analysis (data not shown). Because the individual bands are not resolved at room temperature, all of the intensity between 700 and 900 cm⁻¹ is assumed to arise from the overtones and combination bands. The experimental cross sections are 5.29×10^{-10} and 4.91×10^{-10} Å²/molecule for poplar and spinach plastocyanin, respectively. These cross sections compare well, within our experimental error, to the calculated values of 6.46×10^{-10} and 3.93×10^{-10} Å²/molecule for poplar and spinach plastocyanin, respectively, using eq 3 and the values in Tables 1 and 2. The good agreement between the experimental and calculated overtone and combination band cross sections suggests that little or no Duschinsky rotation of the normal modes occurs, consistent with results in azurin, another Type 1 blue copper protein.^{20,32} Finally, some of the amino acid residue differences, which have been assigned here as the contributing factor to the differences in the resonance Raman spectra in the plastocyanins, simply cannot affect the excited state differently than the ground state, that is, the amino acid differences must act by a through-bond mechanism, which necessarily involves changes in normal modes. For example,

the change of a proton to a methyl group would be more likely to affect the normal modes than any other characteristic of the potential energy surfaces.

This model that has been proposed, wherein the resonance Raman spectrum is sensitive to amino acid changes up to 10 Å from the copper site, requires that there is some delocalization of normal modes into the protein backbone. This requirement follows directly from the experimental evidence that a short pathway, through bonds, must exist between the copper site and the amino acid change. This natural consequence is most clearly seen in the comparison of spinach and poplar *a* plastocyanin, in which a substitution of a methyl group for a proton has a significant effect on the resonance Raman spectrum when it occurs only two amino acids away from a coordinating residue with a short 10 Å through-bond distance. However, in the comparison of zucchini and cucumber plastocyanin, the same substitution occurs over roughly the same through-space distance but on amino acids with an ~60 Å through-bond distance, and no effect on the resonance Raman spectrum is observed. Also, the nature of the amino acid change, a methyl group replacing a proton, argues for a directionally specific type of interaction, such as a change in normal modes, rather than a through-space interaction, such as an electrostatic mechanism.

The model proposed here of delocalized normal modes in plastocyanin is consistent with the emerging picture from isotopically substituted plastocyanins. Frequency shifts and intensity changes of all resonance-enhanced Raman vibrational modes in the 370–450 cm⁻¹ spectral region upon isotopic substitution with ³⁴S, ¹⁵N, and ⁶⁵Cu atoms demonstrate that the copper site internal coordinates are mixed into all of the normal modes of this spectral region.²⁶ The ¹⁵N isotopic substitution, which occurred over all of the protein backbone, however, suggested involvement of more than just the Cu-ligating residues. On the basis of the total isotopic shift over all of the vibrational modes of this spectral region, the authors argued that the normal modes are composed primarily of internal coordinates localized at the copper site. However, a later study, which included more isotopic derivatives further away from the immediate ligand atoms studied previously,⁹ revealed that the number of internal coordinates that make up the resonance-enhanced normal modes is greater than was previously suggested and extends further into the protein from the copper site. Most recently, modeling²⁷ of the copper site and ligated amino acid residues demonstrated that the resonance-enhanced normal modes were delocalized over at least two of the ligated residues, His87 and Cys84, and suggested further involvement of the protein.

Electron Transfer. Plastocyanin is thought to contain two electron transfer pathways, one for the incoming electron to reduce the copper and one for the electron escaping while oxidizing the copper. The first pathway is thought to occur through Cys84 and Tyr83. The second pathway is thought to occur through His87. It is interesting to note that Ala85 sits on the peptide strand between Cys84 and His87, the two ligands involved in the electron transfer function of this protein, and that the resonance Raman spectrum appears to be particularly sensitive to amino acid changes at this position—compare the spectrum of lettuce plastocyanin to other plastocyanins in Figures 1 and 2. Other work from our group has suggested that the resonance Raman intensities are particularly sensitive to amino acid changes along putative electron-transfer pathways within proteins, perhaps reflecting an inherent strong coupling between the active site and those pathways.^{33,34} In addition, previous work has suggested that the resonance-enhanced modes

in this absorption band have some relevance to the electron transport function of the protein.^{9,22–27} The mechanism behind these observations that the resonance Raman spectrum may be reflecting the reaction coordinate for thermal electron transfer in these blue copper proteins requires further study to be elucidated fully. It is our suggestion here that the normal modes of the copper site, which contain protein internal coordinates and are resonance-enhanced by the 600-nm $\pi\pi^*$ transition, represent the reaction coordinate for thermal electron transfer between plastocyanin and its physiological redox partner.

Conclusions

The mixing of protein internal coordinates over distances of ~10 Å from the copper site to internal vibrations localized at the copper site in plastocyanin, a blue copper protein involved in photosynthetic electron transport, is proposed here through comparison of the resonance Raman-derived excited-state dynamics in six plastocyanins with slightly different amino acid composition. This model is supported by experimental evidence directly testing through-space electrostatic vs through-bond mode-mixing mechanisms for the effect of the protein environment on the chromophoric active site vibrational properties. These results imply that a significant portion of the protein not directly involved in binding of redox partners appears to be involved in determining the coordination geometry and redox potential at the copper site and provide insight into the methods nature uses to construct appropriate active sites in proteins.

Acknowledgment. The authors thank R. Morris, A. Dabros, A. Ferrey, S. Scott, K. Mar, and T. Hill for help in the purification of lettuce and zucchini plastocyanins. Financial support was provided by NSERC Canada through the Research Grants-in-Aid program.

Supporting Information Available: Figures 7–10 showing the resonance Raman spectra of zucchini, cucumber, lettuce, and bean plastocyanins at several excitation wavelengths within the ca. 600-nm absorption band and Tables 3–6 listing the experimental and calculated absolute resonance Raman cross sections for zucchini, cucumber, lettuce, and bean plastocyanins for each observed mode at each excitation wavelength. This material is available free of charge via the Internet at <http://pubs.acs.org>.

References and Notes

- (1) Marcus, R. A.; Sutin, N. *Biochim. Biophys. Acta* **1985**, *811*, 265.
- (2) McLendon, G.; Hake, R. *Chem. Rev.* **1992**, *92*, 481.
- (3) Natan, M. J.; Baxter, W. W.; Kuila, D.; Gingrich, D. J.; Martin, G. S.; Hoffman, B. M. In *Electron Transfer in Inorganic, Organic, and Biological Systems*, Bolton, J. R., Mataga, M., McLendon, G., Eds.; American Chemical Society: Washington, DC, 1991; p 201.
- (4) Winkler, J. R.; Gray, H. B. *Chem. Rev.* **1992**, *92*, 369.
- (5) Kirmaier, C.; Weems, D.; Holten, D. *Biochemistry* **1999**, *38*, 11516.
- (6) Farver, O.; Skov, L. K.; Young, S.; Bonander, N.; Karlsson, G. B.; Vanngard, T.; Pecht, I. *J. Am. Chem. Soc.* **1997**, *119*, 5453.
- (7) Sykes, A. G. *Chem. Soc. Rev.* **1985**, *14*, 283.
- (8) Regen, J. J.; Di Bilio, A. J.; Winkler, J. R.; Richards, J. H.; Gray, H. B. *Inorg. Chim. Acta* **1998**, *470*, 275–276.
- (9) Dong, S.; Spiro, T. G. *J. Am. Chem. Soc.* **1998**, *120*, 10434.
- (10) Webb, M. A.; Fraga, E.; Loppnow, G. R. *J. Phys. Chem.* **1996**, *100*, 3278.
- (11) Loppnow, G. R.; Fraga, E. *J. Am. Chem. Soc.* **1997**, *119*, 895–905.
- (12) Fraga, E.; Loppnow, G. R. *J. Phys. Chem. B* **1998**, *102*, 7659.
- (13) Guss, J. M.; Freeman, H. C. *J. Mol. Biol.* **1983**, *169*, 521.
- (14) Boden, N.; Holmes, M. C.; Knowles, P. F. *Biochem. Biophys. Res. Commun.* **1974**, *57*, 845.
- (15) Pleniscar, M.; Bendall, D. S. *Biochim. Biophys. Acta* **1970**, *216*, 192–199.

- (16) Graziani, M. T.; Agro, A. F.; Rotilio, G.; Barra, D.; Mondovi, B. *Biochemistry* **1974**, *13*, 804–809.
- (17) Ramshaw, J. A. M.; Brown, R. H.; Scawen, M. B.; Boulter, D. *Biochim. Biophys. Acta* **1973**, *303*, 269–273.
- (18) Morand, L. Z.; Krogmann, D. W. *Biochim. Biophys. Acta* **1993**, *1141*, 105–106.
- (19) Webb, M. A.; Kwong, C. M.; Loppnow, G. R. *J. Phys. Chem. B* **1997**, *101*, 5062–5069.
- (20) Myers, A. B.; Mathies, R. A. In *Biological Applications of Raman Spectroscopy*; Spiro, T. G., Ed.; Wiley: New York, 1988; Vol. 2, p 1.
- (21) Lee, S.-Y.; Heller, E. J. *J. Chem. Phys.* **1979**, *71*, 4777.
- (22) Han, J.; Adman, E. T.; Beppu, T.; Codd, R.; Freeman, H. C.; Huq, L.; Loehr, T. M.; Sanders-Loehr, J. *Biochemistry* **1991**, *30*, 10904.
- (23) Blair, D. F.; Campbell, G. W.; Schoonover, J. R.; Chan, S. I.; Gray, H. B.; Malmstrom, B. G.; Pecht, I.; Swanson, B. I.; Woodruff, W. H.; Cho, W. K.; English, A. M.; Fry, H. A.; Lum, V.; Norton, K. A. *J. Am. Chem. Soc.* **1985**, *107*, 5755.
- (24) Woodruff, W. H.; Dyer, R. B.; Schoonover, J. R. In *Biological Applications of Raman Spectroscopy*; Spiro, T. G., Ed.; Wiley: New York, 1988; Vol. 3, p 413.
- (25) Qiu, D.; Kilpatrick, L.; Kitajima, N.; Spiro, T. G. *J. Am. Chem. Soc.* **1994**, *116*, 2585.
- (26) Qiu, D.; Dong, S.; Ybe, J. A.; Hecht, M. H.; Spiro, T. G. *J. Am. Chem. Soc.* **1995**, *117*, 6443.
- (27) Qiu, D.; Dasgupta, S.; Kozlowski, P. M.; Goddard, W. A., III; Spiro, T. G. *J. Am. Chem. Soc.* **1998**, *120*, 12791.
- (28) Andrew, C. R.; Han, J.; den Blaauwen, T.; van Pouderoyen, G.; Vijgenboom, E.; Canters, G. W.; Loehr, T. M.; Sanders-Loehr, J. *J. Bioinorg. Chem.* **1997**, *2*, 98.
- (29) Grundler, H.-V.; Schumann, H. D.; Steger, E. *J. Mol. Struct.* **1974**, *21*, 149.
- (30) Vansant, F. K.; van der Veken, B. J.; Herman, M. A. *Spectrochim. Acta A* **1974**, *30A*, 69.
- (31) Chowdhury, A.; Peteanu, L. A.; Webb, M. A.; Loppnow, G. R. *J. Phys. Chem. B* **2001**, *105*, 527.
- (32) Webb, M. A.; Loppnow, G. R. *J. Phys. Chem. B* **1998**, *102*, 8923.
- (33) Webb, M. A.; Loppnow, G. R. *J. Phys. Chem. A* **1999**, *103*, 6283.
- (34) Webb, M. A.; Loppnow, G. R. *J. Phys. Chem. B* **2002**, *106*, 2102.
- (35) Bernstein, F. C.; Koetzle, T. F.; Williams, G. J. B.; Meyer, E. F., Jr.; Brice, M. D.; Rodgers, J. R.; Kennard, O.; Shimanouchi, T.; Tasumi, M. *J. Mol. Biol.* **1977**, *112*, 535–542.
- (36) Guss, J. M.; Bartunik, H. D.; Freeman, H. C. *Acta Crystallogr.* **1992**, *B48*, 790.